

# LTOS: Layout-controllable Text-object Synthesis via Adaptive Cross-attention Fusions

1<sup>st</sup> Xiaoran Zhao

National University of Defense Technology

2<sup>nd</sup> Tianhao Wu

Nanyang Technological University

3<sup>rd</sup> Yu Lai

National University of Defense Technology

4<sup>th</sup> Zhiliang Tian

National University of Defense Technology

5<sup>th</sup> Zhen Huang

National University of Defense Technology

6<sup>th</sup> Yahui Liu

Huawei Technologies Ltd

7<sup>th</sup> Zejiang He

National University of Defense Technology

8<sup>th</sup> Dongsheng Li

National University of Defense Technology

**Abstract**—Controllable text-to-image generation synthesizes visual text and objects in images with certain conditions. However, existing visual text rendering and layout-to-image generation tasks focus on single modality generation or rendering, leaving yet-to-be-bridged gaps between the approaches correspondingly designed for each of the tasks. In this paper, we introduce a unified task called layout-controllable text-object synthesis (LTOS), which merges text rendering and layout-based object generation. We construct a layout-aware text-object synthesis dataset for LTOS task, containing well-aligned labels visual text and object information. We also propose a layout-controllable text-object adaptive fusion (TOF) model, which generates images with legible visual text and plausible objects. Specially, we construct a visual-text rendering to synthesize text and employ an object-layout control module to generate objects while integrating the two modules to harmoniously generate and integrate text and objects in images. To enhance the image-text integration, we propose a self-adaptive cross-attention fusion that forces the image generation to attend more to important text spans. Within such a fusion, we use a self-adaptive learnable factor to learn to control the influence of cross-attention outputs. Experiments show that our model excels the SOTA in LTOS, text rendering, and layout-to-image tasks. We release our dataset and codes<sup>1</sup>.

**Index Terms**—Text rendering, Text-object synthesis

## I. INTRODUCTION

Controllable text-to-image (T2I) generation [1] synthesizes text contents and objects on an image, which makes the generated images harmoniously juxtaposed with visual text [2] and has many applications including emoji crafting [3] and poster design [4]. Text rendering and layout-to-image, as two popular tasks, have appealed to extensive research interests. (1) **Text rendering** in images refers to generating clear and legible text in images, which needs to be visually compatible with the image in terms of texture and depth. Latest methods [5]–[7] typically encode the text input into an image with the backbone of LDMs [8] or ControlNet [9] to achieve high-quality text rendering. (2) **Layout-to-image generation** task is to generate an image according to a given layout map such as bounding boxes with object categories [10] or a semantic segmentation map [11], [12]. The core of this task is to

accurately control the location of generated objects, which can be seen as the reverse task of object detection [13]. Despite the

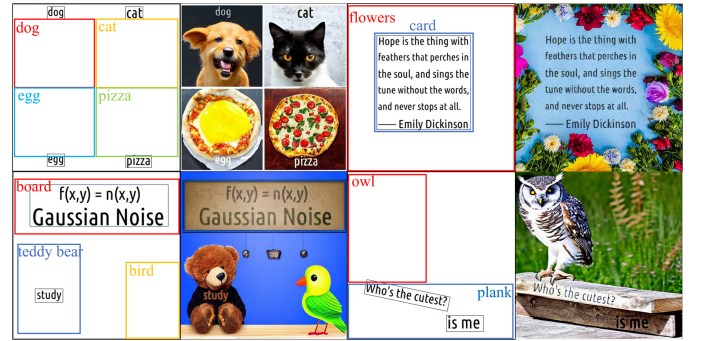


Fig. 1. Our model TOF’s examples. Given predefined visual text and object information, TOF generates object following the layout map while rendering text consistent to image’s depth, texture, and geometry.

booms on the two tasks, the majority of these approaches can only accurately control one singular modality: text rendering caters more to the quality of the generated visual text and controls objects simply with prompts, failing to define the positions of the objects; layout-to-image generation focuses on controlling objects, ignoring the clarity and rationale of the generated visual text. Such differentiation in focus led to a significant and yet-to-be-bridged gap between the design of methods to control text and objects.

To mitigate this challenge, we integrate the aforementioned two mainstream tasks - text rendering and layout-to-image generation - into a singular task: layout-controllable text-object synthesis (LTOS). LTOS’s objective is to generate an image with visual text, where the location of the objects and text can be accurately controlled by providing a layout map together with object categories and visual text information. Due to the lack of datasets containing both textual and object layout information for this task, we develop a layout-aware text-object synthesis (LTOS) dataset. It contains well-aligned multi-modal label information including image captions (prompts), word-level visual text and object bounding boxes with category

<sup>1</sup><https://anonymous.4open.science/r/TOF-D5EE>

labels. LTOS dataset is easily expanded with a three-step workflow and has high quality comparable to the real dataset.

Based on our dataset, we further propose a layout-controllable text-object adaptive fusion (TOF) model that synthesizes images with high-quality object and visual text conditioned on the given object layouts and text contents. TOF consists of 1) an object-layout control module, 2) a visual-text rendering module, and 3) a text-object self-adaptive fusion module. Given the spatial layout information of objects (i.e. object categories with matching bounding boxes), our *object-layout control module* generates images with each object placed at the predetermined location; Our *visual text rendering module* customizes the instructions for rendering text layouts with multi-regional and multi-directional. To harmoniously integrate text content and image objects, we integrate the above two modules to jointly control layout of visual text and objects. To balance the visual text rendering and object-layout control on the integration, we propose a *text-object self-adaptive fusion module* to select important text information to image generation via a cross-attention mechanism [14]. To absorb the cross-attention outputs, we employ a self-adaptive learnable factor that learns to fetch the influence of cross-attention outputs for image generation. Experimental results on LTOS dataset show that our method excels SOTA baselines on both text rendering and layout-to-image tasks. Our contributions are: (1) We merge text rendering and layout-to-image generation tasks and define an unified task: layout-controllable text-object synthesis (LTOS) to synthesize text and object into an image. (2) We construct a layout-aware text-object synthesis dataset for LTOS. (3) We propose a layout-controllable text-object adaptive fusion (TOF) model for LTOS. It customizes the shape and text layout and controls text-object synthesis.

## II. METHOD

As Fig. 2, our model consists of a visual-text control module and an object-layout control module for text-object integration control (Sec. II-C). Further, we propose a text-object self-adaptive fusion to balance text and object (Sec. II-D).

### A. Task formulation

For our LTOS task, we denote LTOS’s input  $I$  consists of a text prompt with image content  $\mathbf{c}$ , a layout map  $O$  consisting of object categories (with its bounding boxes), a glyph image  $G$  including text content, position, and shape information,  $I = \langle \mathbf{c}, O, G \rangle$ . Considering an image with  $n$  objects and  $m$  text regions,  $I = \langle \mathbf{c}, \{(o_1, b_{o_1}), \dots, (o_n, b_{o_n})\}, \{(t_1, g_{t_1}), \dots, (t_m, g_{t_m})\} \rangle$ , where  $o_i$  and  $t_j$  denote the object category information and the visual text content respectively,  $b_{o_i}$  is the bounding box for  $o_i$  and  $g_{t_j}$  is the corresponding glyph region for  $t_j$  ( $1 \leq i \leq n, 1 \leq j \leq m$ ). Given the input, our target is generating an image satisfying 1) the generated objects are within each bounding box, consistent to the specified categories and the text descriptions; 2) the visual text formatting (i.e., position, font size, and distortion) follows the exact guidance of the glyph image; and 3) the rendered text

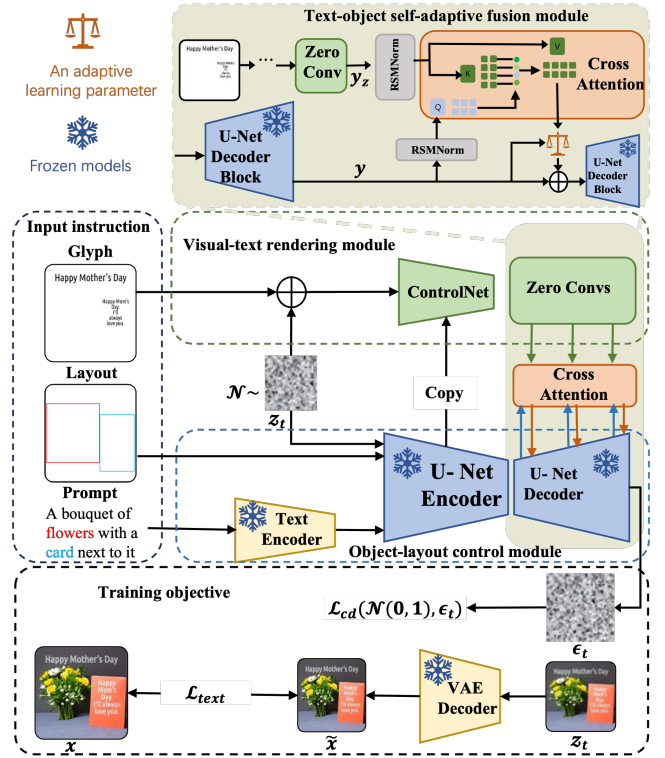


Fig. 2. TOF framework. Given the input with a prompt, a glyph image, and a layout map, TOF achieves controllable text-object synthesis.

is clear and seamlessly integrated with the generated image in terms of depth, texture and geometry.

### B. Dataset Construction

Existing datasets with both visual-text and object layout aren’t available. Besides, datasets used for text rendering face some limitations: 1) Each text area filtered is more than 10% of the entire image area [6], [15]; 2) visual text appears in center areas of the image and rarely in border areas [16]. Hence, it leads to potential issues including the incapability to generate tiny-font text and high-quality visual text in border areas.

Considering the limitations, we propose a layout-aware text-object synthesis dataset, a multi-modal dataset with comprehensive well-aligned labels in both visual text and object. We choose the Flickr30K [17] dataset as the basis for embedding textual information at appropriate places within images, and the Flickr30K Entities dataset [18] to supplement object category annotated bounding boxes. However, Flickr30K doesn’t include visual text information, which is crucial for our task. Fortunately, SynthText [19] provides a potential solution by enriching the data with coarse visual text rendering.

The dataset construction involves three steps. **Step 1:** Select regions suitable for text rendering by using texture and depth information of images; **Step 2:** Set filtering rules to generate text as required and color the text based on Color-model [19]; **Step 3:** Perform Poisson image editing [20] to blend the text into the scene. The filtering rules in step 2 includes: 1) Text region number ranges in [1, 8]; 2) The number of text lines

ranges in [1, 8]; 3) The text is generated in random regions considering suitable for image's text rendering; 4) Each text region exceeds 2% of the image in length and width, with a minimum area of 5% of the entire image; 5) Text is randomly rotated, twisted, bolded, and bordered. While following this workflow, we noticed that the background of text regions recognized as suitable for text rendering were too cluttered. To address the issues, we first replaced the original depth maps by implementing recent Zoedepth [21] to estimate more precise depth and then applied PPOCRv3 [22] to filter out all the images whose textual content is not recognizable, i.e. containing low-quality renderings. These optimizations enable stable and higher-quality text rendering, comparable to the real dataset in terms of depth, texture, and geometry.

LTOS dataset includes 228k samples. Each sample has: 1) an image with rendered text, 2) a caption of the image used as the prompt, 3) grounded word-level text annotations with enough information to obtain the corresponding glyph image, and 4) grounded object annotations. LTOS has some fine-grained attributes: depth of the visual text, multiple thicknesses, multiple text regions, and different rotation angles.

### C. Text-object integration control model

To handle LTOS task, we propose a visual-text rendering module and an object-layout control module to render text on the image and generate images with objects conditioned on specific layouts. (1) **Visual-text rendering module** generates visual text with multi-regional and multi-directional layouts and injects the feature of glyph images as conditions to guide the text-rendered images. Inspired by GlyphControl [7] and AnyText [6], we employ a trainable ControlNet [9] to achieve text rendering for its capability to control the geometric structures accurately. But this module hardly controls the accurate layout of the generated objects, especially facing with multiple objects. (2) To control the generation of objects more precisely, we propose a **Object-layout control module** extracts features from the object layout map  $O$  based on GLIGEN [23], and generate images with the layout. The above mechanism achieves controllable visual-text rendering and object generation by connecting the ControlNet-based text rendering to LDM-based object-layout control.

### D. Text-object self-adaptive fusion module

To better integrate text and objects, we propose a text-object self-adaptive fusion that adaptively bridges the visual-text rendering and object-layout control. The motivation is that the aforementioned module (Sec. II-C) encounter two issues: (1) it is difficult to balance text rendering and object generation. Over-training leads to the distortion of some generated objects, while under-training makes it hard to render clear and legible text. (2) rendering multiple text areas on diverse objects results in blurred and unclear visual text in images. To mitigate this issue, we propose to bridge text and object via adaptive cross-attention, where (1) the cross-attention fetches textual information to help image generations and (2) a self-adaptive learnable factor adaptively learns to leverage the information

from the cross-attention. The cross-attention consists of three sub-modules. **Cross-attention backbone** follows the vanilla cross-attention [24]. As shown in Fig. 2, each block  $B$  in the object-control module corresponds to a trainable copy block with a zero-convolution layer, together denoted as  $B_z$ , in the visual-text module. we inject cross-attention layers between the output of  $B$  and  $B_z$ , denoted as  $y$  and  $y_z$  respectively. The cross-attention layer takes  $y$  and  $y_z$  as input and output a feature vector  $y_a$  that combines the visual text and object information. **RMSNorm operation** enables the rapid convergence [25] in our cross-attention backbone. We applied RMSNorm to the input of cross-attention  $y$  and  $y_z$  (i.e. the output of object-control and zero-convolution). The RMSNorm's outputs act as the cross-attention's input as:  $y_a = \text{cross-attention}(\text{RMSNorm}(y), \text{RMSNorm}(y_z))$ . **Self-adaptive learnable factor** learns to decide how much information from cross-attention is used (i.e. influence of cross-attention's output  $y_a$ ). It allows the model to adjust the weights of additional visual text  $y_a$  and object  $y$ . We apply  $\tanh(\cdot)$  the learnable factor  $\alpha$  to control its range in  $[0, 1)$ . To linearly weighted integrate  $y_a$  and  $y$ , we element-wise sum up the object  $y$  and  $y_a$  adjusted by the factor as  $\alpha$ . Then, we concatenate the summation with  $y^2$  as the output of this module  $y_f$ , formalized as  $y_f = \text{concat}(y, y + \tanh(\alpha) * y_a)$ .

### E. Training objective

The training process is as follows: we feed the given input image  $x \in \mathbb{R}^{H \times W \times 3}$ , into a pre-trained VAE [26] to get its latent vector  $z_0 \in \mathbb{R}^{h \times w \times c}$ . In the object-layout control module, each gated self-attention layer's input is denoted as  $z_b$ . In the visual-text rendering module, we extract its feature as  $z_g$  [27], [28]. During the diffusion process, we sample a time  $t \sim \text{Uniform}(0, 1000)$  and a Gaussian noise  $\epsilon \sim \mathcal{N}(0, 1)$ , and corrupt  $z_0$  to generate noisy latent images  $z_t$ . Our training objective consists of: (1) controllable diffusion loss  $\mathcal{L}_{cd}$ . Our model employs a network  $\epsilon_\theta$  to estimate the noise that has been introduced to the latent image  $z_t$  [29] as:

$$\mathcal{L}_{cd} = \mathbb{E}_{z_0, z_b, z_g, t, \epsilon \sim \mathcal{N}(0, 1)} [\|\epsilon - \epsilon_\theta(z_t, z_b, z_g, t)\|_2^2] \quad (1)$$

(2) Text perceptual loss  $\mathcal{L}_{text}$ . Inspired by [6], we minimize the distance between rendered text in generated image  $\tilde{x}$  and the ground truth image  $x$ . Specifically, with our grounded word-level text annotations, we crop each  $x$  and  $\tilde{x}$  pair into sub-images  $\mathcal{S} = \{s_1, \dots, s_j\}$  and  $\mathcal{S}' = \{s'_1, \dots, s'_j\}$  with one text region in each  $s_*$ . We feed  $\mathcal{S}$  and  $\mathcal{S}'$  into the PP-OCRv3 model [22] and calculate the mean squared error [30] (MSE) between the features  $f_i, f'_i \in \mathbb{R}^{h \times w \times c}$  from the last fully connected layer:  $\mathcal{L}_{text} = \sum_i \frac{\phi(t)}{hw} \cdot \sum_{h,w} \|f_i - f'_i\|_2^2$ , where  $\phi(t)$  is a weight adjustment [6] same as the coefficient of diffusion process in [29]. The overall training objective is  $\mathcal{L} = \mathcal{L}_{cd} + \lambda * \mathcal{L}_{text}$ , where  $\lambda$  balances  $\mathcal{L}_{cd}$  and  $\mathcal{L}_{text}$ .

## III. EXPERIMENT

a) **Experimental settings:** Our backbone is based on GLIGEN [23]. We initialize visual-text rendering module

<sup>2</sup>Concatenating  $y$  and  $y_a$  instead of summing generates distorted objects.

TABLE I

TOF’S RESULTS COMPARED TO BASELINES AND ANALYSIS OF FUSION CROSS-ATTENTION LAYERS. \* DENOTES FINETUNING ON LTOS DATASET. WE REPORT OCR, ACC, NED AND AP SCORES.

Method	OCR, ACC $\uparrow$	NED $\uparrow$	AP $\uparrow$
TextDiffuser [15]	0.2551	0.4824	-
GlyphControl* [7]	0.3601	0.5404	-
AnyText [6]	0.1732	0.3274	-
GLIGEN [23]	0.0018	0.0092	0.4958
Our TOF	<b>0.4353</b>	<b>0.6325</b>	<b>0.5658</b>
4-layer Sparse	0.4039	0.5956	0.4791
2-layer Dense	0.4203	0.6161	0.4571
7-layer Dense	0.4115	0.6015	0.4671
10-layer Dense	0.3533	0.4402	0.4710
4-layer Dense (Our TOF)	<b>0.4353</b>	<b>0.6325</b>	<b>0.5658</b>

with pre-trained “bounding box + text” weights. Our dataset consists of 217,820 training and 11,113 testing samples. For diffusion, we set the downsampling factor  $f = 8$ , and the latent dimension is  $64 \times 64 \times 4$ . We train the model for 1.3 M iterations with batch size 24. Since LTOS is a novel designed task, we mainly compare our model to the following SOTA baselines: including layout-to-image generation model GLIGEN [23]<sub>CVPR’22</sub>. We compare our model to text rendering baselines with TextDiffuser [31]<sub>NeurIPS’23</sub>, AnyText [6]<sub>ICLR’24</sub> and GlyphControl [7]<sub>NeurIPS’23</sub>. We use three metrics: 1) OCR, Acc [22], the word-level accuracy of rendered texts; 2) Normalized Edit Distance (NED) [32], the similarity between two strings; 3) AP [33], the accuracy of object generation.

b) **Main results:** As Table I, our model significantly outperform all state-of-the-art baselines on the benchmark dataset in all metrics (+7.52% on OCR, ACC and +9.21% on NED). AnyText performs bad in OCR, ACC and NED, since it hardly automatically wraps and many multi-line texts in the LTOS dataset. Because the text rendered by GlyphControl is only rotated up to 20 degrees clockwise or counterclockwise, we fine-tuned on the LOST dataset, the results were still not ideal compared to our model.

c) **Ablation studies:** In Table II, removing any of the modules results in worse results. Row 1 and 4 verify the effectiveness of *text-object self-adaptive fusion*. Row 2 ascertains the validity of the *self-adaptive mechanism* in Sec. II-D. Row 3 in Table II suggests that *text perceptual loss* enhances the quality of text generation.

d) **Analyses on attention-layers:** We test the results with different numbers and settings of injecting cross-attention layers (**4-layer Dense:** four layers after the 0-th to 3-rd zero-convolution layers; **4-layer Sparse:** four layers after the 0-th, 3-rd, 6-th and 9-th zero-convolution layers) in Table I. It suggests that increasing the number of layers doesn’t necessarily lead to better results. Instead, over-introduction of layers can lead to significant results degradation. Results show the 4-layer Dense leads to best results, which is used in our paper.

e) **Qualitative results:** Our qualitative results compared with baselines and widely used text-to-image generation APIs

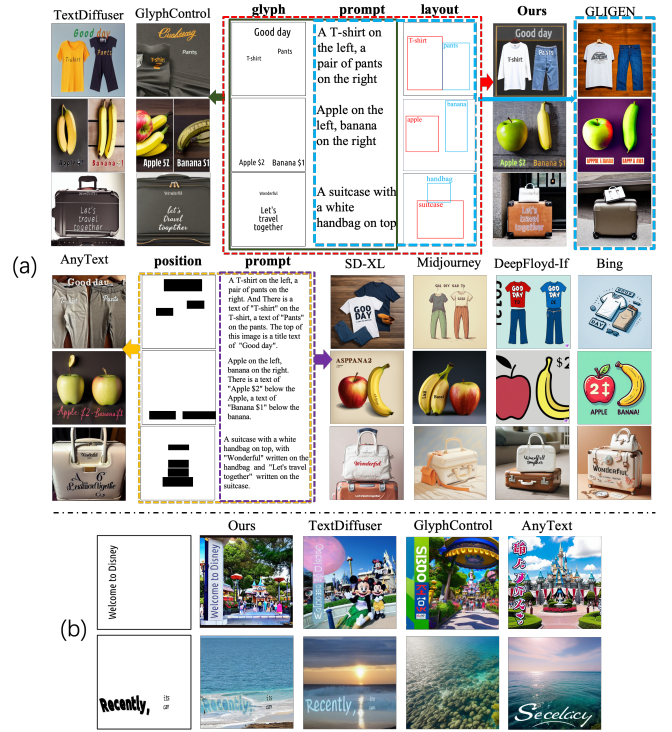


Fig. 3. Qualitative comparison of TOF and the baselines. Due to the certain differences between our input and baselines, we keep the input to be the same based on the input format accepted by all models and implementation details.

TABLE II  
ABLATION RESULTS OF TOF ON LTOS DATASET.

Cross-Attention	$\mathcal{L}_{\text{text}}$	$\alpha$	OCR, ACC $\uparrow$	NED $\uparrow$	AP $\uparrow$
$\times$	$\checkmark$	$\times$	0.4014	0.5951	0.4501
$\checkmark$	$\checkmark$	$\times$	0.4218	0.6177	0.4662
$\checkmark$	$\times$	$\checkmark$	0.4268	0.6203	0.5003
$\checkmark$	$\checkmark$	$\checkmark$	<b>0.4353</b>	<b>0.6325</b>	<b>0.5658</b>

(SD-XL, Midjourney, DeepFloyd IF and Bing Image Creator) are visualized in Fig. 3 (a). It shows that our method renders more legible, clearer visual texts and plausible objects at the predefined positions. Our model supports arbitrary rotation of text area, tiny font and different thicknesses of font in Fig. 3 (b). We observed notable limitations in the baselines. AnyText cannot automatically wrap resulting in garbled text. TextDiffuser and GlyphControl fail to render tiny-font text and some special characters. Further, they all sometimes generate objects of the wrong categories or omit objects.

#### IV. CONCLUSION

We define an unified task LTOS accurately controlling visual text and object generation and propose the LTOS dataset. Further, we propose a novel TOF model with a text-object self-adaptive cross-attention fusion module balancing text and object synthesis. Experiments show that TOF excels SOTA baselines for text rendering maintaining comparable results to the object generation model.



## REFERENCES

- [1] P. Cao, F. Zhou, Q. Song, and L. Yang, "Controllable generation with text-to-image diffusion models: A survey," *arXiv preprint arXiv:2403.04279*, 2024.
- [2] L. Auvil, E. Grois, X. Llorà, G. Pape, V. Goren, B. Sanders, B. Acs, and R. McGrath, "A flexible system for text analysis with semantic network," *Digital Humanities*, pp. 17–20, 2007.
- [3] C. K. Suryadevara, "Emojify: Crafting personalized emojis using deep learning," *International Journal of Innovations in Engineering Research and Technology*, vol. 6, no. 12, pp. 49–56, 2019.
- [4] H. Huo, F. Wang *et al.*, "A study of artificial intelligence-based poster layout design in visual communication," *Scientific Programming*, vol. 2022, 2022.
- [5] Y. Zhao and Z. Lian, "Udifftext: A unified framework for high-quality text synthesis in arbitrary images via character-aware diffusion models," *arXiv preprint arXiv:2312.04884*, 2023.
- [6] Y. Tuo, W. Xiang, J.-Y. He, Y. Geng, and X. Xie, "Anytext: Multilingual visual text generation and editing," in *The Twelfth International Conference on Learning Representations*, 2023.
- [7] Y. Yang, D. Gui, Y. Yuan, W. Liang, H. Ding, H. Hu, and K. Chen, "Glyphcontrol: Glyph conditional control for visual text generation," *Advances in Neural Information Processing Systems*, vol. 36, 2024.
- [8] R. Rombach, A. Blattmann, D. Lorenz, P. Esser, and B. Ommer, "High-resolution image synthesis with latent diffusion models," in *Proceedings of the IEEE/CVF Conference on Computer Vision and Pattern Recognition*, 2022, pp. 10 684–10 695.
- [9] L. Zhang, A. Rao, and M. Agrawala, "Adding conditional control to text-to-image diffusion models," in *Proceedings of the IEEE/CVF International Conference on Computer Vision*, 2023, pp. 3836–3847.
- [10] L. H. Li, P. Zhang, H. Zhang, J. Yang, C. Li, Y. Zhong, L. Wang, L. Yuan, L. Zhang, J.-N. Hwang *et al.*, "Grounded language-image pre-training," in *Proceedings of the IEEE/CVF Conference on Computer Vision and Pattern Recognition*, 2022, pp. 10965–10975.
- [11] Y. He, R. Salakhutdinov, and J. Z. Kolter, "Localized text-to-image generation for free via cross attention control," *arXiv preprint arXiv:2306.14636*, 2023.
- [12] T.-Y. Lin, M. Maire, S. Belongie, J. Hays, P. Perona, D. Ramanan, P. Dollár, and C. L. Zitnick, "Microsoft coco: Common objects in context," in *Computer Vision—ECCV 2014: 13th European Conference, Zurich, Switzerland, September 6–12, 2014. Proceedings, Part V 13*. Springer, 2014, pp. 740–755.
- [13] Z. Zou, K. Chen, Z. Shi, Y. Guo, and J. Ye, "Object detection in 20 years: A survey," *Proceedings of the IEEE*, vol. 111, no. 3, pp. 257–276, 2023.
- [14] A. Vaswani, N. Shazeer, N. Parmar, J. Uszkoreit, L. Jones, A. N. Gomez, L. Kaiser, and I. Polosukhin, "Attention is all you need," *Advances in Neural Information Processing Systems*, vol. 30, 2017.
- [15] J. Chen, Y. Huang, T. Lv, L. Cui, Q. Chen, and F. Wei, "Textdiffuser: Diffusion models as text painters," *Advances in Neural Information Processing Systems*, vol. 36, 2024.
- [16] J. Ma, M. Zhao, C. Chen, R. Wang, D. Niu, H. Lu, and X. Lin, "Glyphdraw: Learning to draw chinese characters in image synthesis models coherently," *arXiv preprint arXiv:2303.17870*, 2023.
- [17] P. Young, A. Lai, M. Hodosh, and J. Hockenmaier, "From image descriptions to visual denotations: New similarity metrics for semantic inference over event descriptions," *TACL*, vol. 2, pp. 67–78, 2014.
- [18] B. A. Plummer, L. Wang, C. M. Cervantes, J. C. Caicedo, J. Hockenmaier, and S. Lazebnik, "Flickr30k entities: Collecting region-to-phrase correspondences for richer image-to-sentence models," *IJCV*, vol. 123, no. 1, pp. 74–93, 2017.
- [19] A. Gupta, A. Vedaldi, and A. Zisserman, "Synthetic data for text localisation in natural images," in *Proceedings of the IEEE/CVF Conference on Computer Vision and Pattern Recognition*, 2016, pp. 2315–2324.
- [20] P. Pérez, M. Gangnet, and A. Blake, "Poisson image editing," in *Seminal Graphics Papers: Pushing the Boundaries, Volume 2*, 2023, pp. 577–582.
- [21] S. F. Bhat, R. Birkel, D. Wofk, P. Wonka, and M. Müller, "Zoedepth: Zero-shot transfer by combining relative and metric depth," *arXiv preprint arXiv:2302.12288*, 2023.
- [22] C. Li, W. Liu, R. Guo, X. Yin, K. Jiang, Y. Du, Y. Du, L. Zhu, B. Lai, X. Hu *et al.*, "Pp-ocrv3: More attempts for the improvement of ultra lightweight ocr system," *arXiv preprint arXiv:2206.03001*, 2022.
- [23] Y. Li, H. Liu, Q. Wu, F. Mu, J. Yang, J. Gao, C. Li, and Y. J. Lee, "Gligen: Open-set grounded text-to-image generation," in *Proceedings of the IEEE/CVF Conference on Computer Vision and Pattern Recognition*, 2023, pp. 22 511–22 521.
- [24] A. V. S. Parmar, "Attention is all you need," in *Proceedings of the International Conference on Neural Information Processing Systems*, 2017.
- [25] B. Zhang and R. Sennrich, "Root mean square layer normalization," *Advances in Neural Information Processing Systems*, vol. 32, 2019.
- [26] D. P. Kingma and M. Welling, "Auto-encoding variational bayes," *arXiv preprint arXiv:1312.6114*, 2013.
- [27] A. Bansal, H.-M. Chu, A. Schwarzschild, S. Sengupta, M. Goldblum, J. Geiping, and T. Goldstein, "Universal guidance for diffusion models," 2023.
- [28] S. Kim, J. Lee, K. Hong, D. Kim, and N. Ahn, "Diffblender: Scalable and composable multimodal text-to-image diffusion models," 2023.
- [29] J. Ho, A. Jain, and P. Abbeel, "Denoising diffusion probabilistic models," *Advances in Neural Information Processing Systems*, vol. 33, pp. 6840–6851, 2020.
- [30] T. Chai, R. R. Draxler *et al.*, "Root mean square error (rmse) or mean absolute error (mae)," *Geoscientific model development discussions*, vol. 7, no. 1, pp. 1525–1534, 2014.
- [31] L. Zhang, X. Chen, Y. Wang, Y. Lu, and Y. Qiao, "Brush your text: Synthesize any scene text on images via diffusion model," in *Proceedings of the AAAI Conference on Artificial Intelligence*, vol. 38, no. 7, 2024, pp. 7215–7223.
- [32] E. Marzal, A. Vidal, "Computation of normalized edit distance and applications," *Pattern Analysis and Machine Intelligence, IEEE Transactions on*, pp. 926–932, 1993.
- [33] Z. Li, J. Wu, I. Koh, Y. Tang, and L. Sun, "Image synthesis from layout with locality-aware mask adaption," in *Proceedings of the IEEE/CVF International Conference on Computer Vision*, 2021, pp. 13 819–13 828.